Inter-satellites Optical Communication Systems for Defense - I

João Miguel Madeira Trindade, Military Academy/IST

***Abstract*— Satellite communication systems are increasingly more used by the society in many applications, and its development is a high priority for the scientific community. The need for increasing bandwidth to satisfy the users' needs, makes inter-satellites Free Space Optics (FSO) communication preferred instead of traditional radio frequency links.**

The inter-satellites communication links with high bit rates and low power is a determining factor in the performance of these systems. As such communications occur over long distances and high altitude orbits, optical sources with highly collimated and coherent beams are needed in order to ensure a better link between the transmitter and the receiver with low emission power.

This paper involves the development of two experimental blocks for implementing an inter-satellite optical communication system using a semiconductor laser type. It aims at the definition and analysis of the elements of the two circuits, at the transmitter subsystem and includes the design for the production of printed circuit boards (PCB). Moreover, experimental tests were performed to validate the results obtained in the simulations.

***Index Terms*— Satellites, Optical Communications, Transmitter Subsystem, Semiconductor Laser.**

I. Introduction

THE demand for diversified services, such as the use of high speed internet, videoconference and watching programs or videos directly on the Internet (streaming) has resulted in a dramatic increase of the bandwidth required, as the data rate transmission is determined by the available bandwidth [1], [2].

Satellites have nowadays several applications of great importance to the society, such as in telecommunications, in weather forecast and in earth's surface observation, on GPS coordinates navigation (Global Positioning System), and even in space research. On the military scope the mentioned applications gain a higher importance in recognition and surveillance as they are used in the theatre of operations (TO). The information collected in real time may represent and advantage to the military leadership enabling their decision making [2].

The wide spectrum of the optical communications (without regulation so far), unlike the RF communications, represent an additional advantage due to the possibility of data rate transmission of the order of dozens of Gbps [1].

A crucial device to establish the communication between the satellites is the optical source. The semiconductor lasers are often considered ideal sources of transmission due to their high efficiency in the conversion of electrical into optical power, their small size, their easy integration and their low energy consumption. Their low cost is also a reason to select them as the optical source to be used [3], [4].

The purpose of this paper is to define a transmitter subsystem, operating at optical frequencies, that may be integrated in a satellite intercommunication system, simulate the transmitter subsystem, and build and test the several blocks that constitute this subsystem.

II. State of Art of the Optical Communications Inter-satellites

A. Satellite Systems Evolution

The development of lasers since the 60's of the XXth century, triggered the interest of international agencies of this technology. The European Space Agency (ESA) developed the first studies for the use of lasers in inter-satellite communications. In the beginning of 1991 the first unidirectional inter-satellite communication link was established through the program SILEX. The connection was established between the Pastel optical terminals, on board of the French ground observation satellite SPOT-4 and OPALE, installed in the European communications satellite ARTEMIS [5], [6]. The satellites SPOT-4 and ARTEMIS were set in a low earth orbit (LEO) and in a geostationary orbit, respectively. The distance between them is approximately 45000 km and while SPOT-4 transmitted images at 50 Mbps rate to ARTEMIS, this satellite would retransmit them to Earth almost in real time. To establish this connection a laser with a power transmission of 60 mW was used, with a wavelength of 0.8 μm and OOK modulation [4], [7].

In 2008 a successful demonstration of an optical inter-satellite connection (between satellites TerraSAR-X and NFIRE) on the low earth orbit was established. The LCTs enabled the increase of the users' data traffic compared to the radiofrequency connections and they are, nowadays, the most used modules in the industry to establish inter-satellite optical communications [4], [8].

B. Conditioning factors to the inter-satellites communication

The satellites can be grouped according to their purpose and orbit type.

Regarding the purpose, there are communication satellites which are responsible for voice, TV and Internet transmission.

There are also meteorological, scientific, navigation, earth observation and military satellites. Military satellites are essential in navigation assistance and in the positioning of military forces as well as in surveillance and recognition tasks, minimizing the enemy's surprise effect [9].

In what concerns the type of orbit, there are three of satellites according to their distance from the Earth. In Pic. 1 the three types of orbits are presented.

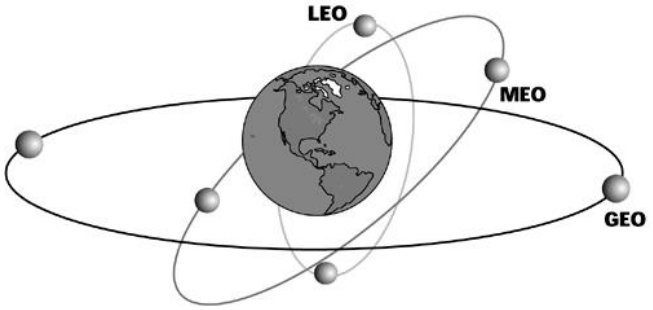

Picture 1 - Three types of orbits

- Low Earth Orbit (LEO): which corresponds to a distance of 180 to 2000 km from the earth's surface. This type of satellites is ideal for military observations, for meteorological data collection and also for communications. They consume less operation energy and they have less launching costs.
- Medium Earth Orbit (MEO): corresponding to 2000 km to 25800 km above the earth's surface. These are generally navigation (GPS), communication and scientific satellites. Their coverage area is wider than LEO's.
- Geostationary Earth Orbit (GEO): they orbit the Earth at a 35800 km distance and their orbital period is 24 hours [10], [11]. They cover a wider area, but they are big devices, expensive and which demand a lot of energy to be launched into space.

In general, the orbits at a higher altitude are more stable due to less interference caused by atmospheric density and by gravitational fluctuations. The gravitational fields of the celestial bodies (such as the Moon and the Sun), the solar radiations and the centrifugal force effect generated by the Earth's rotation movement can affect the orbital stability of the satellites [12].

C. Basic Parameters of the inter-satellites communication systems

The optical communications established between satellites occur mainly in the exosphere atmospheric layer (above 500 km) and although the temperatures reach as much as 1000 ºC, there is no danger of overheating for the satellites as the atmosphere is extremely rarefied causing a very low heat exchange. This way there is no attenuation caused by the atmosphere and it is considered that the electromagnetic field generated by the transmitter propagates almost in vacuum.

In an optical communication system there must be communication between the transmitter and the receiver. The power of the optical signal transmitted is affected by many factors before reaching the receiver. These factors include loss of connection route in the free space (l_s), pointing losses (l_p) and background radiation. The pointing losses are a result of the difference between the beam direction and the satellite position. Regarding the losses due to the divergence of the beam, they can be calculated considering the opening angles (θ_T *and* θ_R) and the diameter of the antenna (D_T *and* D_R) [5], [13].

The performance of this system can be obtained through the power flow equation. The power of the signal received (p_R) [W] depends on the power transmitted (p_T) [W], on the transmitting antenna gain (p_T), on the receiving antenna gain (g_R), on the route losses in the free space and on the transmitter (l_{pt}) and the receiver (l_{pr}) pointing losses.

$$p_R = p_T . g_T . l_{pt} . l_s . g_R . l_{pr} \quad (1)$$

The antenna gain (g) depends on the lens optical efficiency (η) and the antenna opening diameter (D) [m] as given by:

$$g = \eta \left(\frac{\pi . D}{\lambda}\right)^2 \quad (2)$$

This way, the transmitting (g_T) and receiving (g_R) gain is calculated considering the opening diameter of the transmitting and receiving antennas, respectively D_T *and* D_R . The opening angles can be calculated through:

$$\theta = 2.24 \frac{\lambda}{D} \quad (3)$$

where θ_T *and* θ_R are the opening angles of the transmitting and receiving antenna in radians. The pointing losses are given by:

$$l_p = e^{-g\theta^2} \quad (4)$$

The route losses in free space (l_s) depend on the length of the link (d) [m] and are given by:

$$l_s = \left(\frac{\lambda}{4\pi . d}\right)^2 \quad (5)$$

In general, considering the analysis of the above expressions, the advantages of the FSO system are a result of the basic characteristics of the laser beam. As can be inferred from (2) and (5), for higher frequencies higher transmitting and receiving gains are obtained and less free space losses occur [5], [13].

III. CHARACTERISTICS OF THE TRANSMITTING SUBSYSTEM

A. Blocks description and diagram

The current FSO systems operate typically in wavelengths in the near infrared spectrum, between 800 and 1600 nm. There are some special windows of wavelengths of operation, more specifically 850, 1310 and 1550 nm. The 1310 and 1550

windows match the standard transmitting windows of the optical fiber communication systems, so the majority of the FSO commercial systems operate in these two windows in order to use the most common components. The Ultra-Violet (UV) wavelength was recently considered for the FSO systems, because apart from being less subject to pointing errors and to beam interference it has the advantage of being less sensible to interferences caused by background radiation [14], [15]. Pic. 2 shows the electromagnetic spectrum where we can observe the ultraviolet radiation, visible and infrared areas.

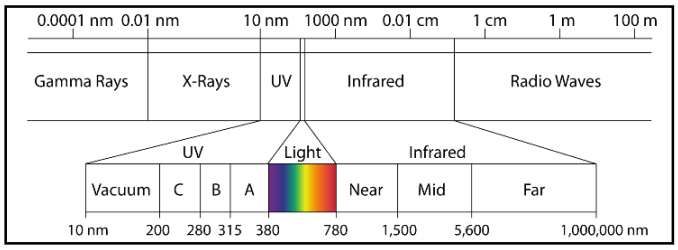

Picture 2 - Electromagnetic Spectrum

The transmitting system is composed by the optical source, the modulator, the optical amplifier and in the end there is the optical beam, as we can see in Pic. 3. The channel encoding can be performed optionally before modulation; this way the bits generated by the source are first codified and later modulated. In order to increase the optical intensity of the laser beam which was formerly modulated, an optical amplifier can be used. Then, the light beam is transmitted through an optical antenna.

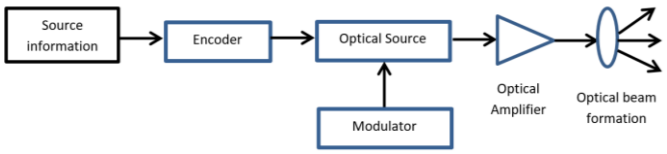

Picture 3 - Block diagram of the optical transmitter

The optical source used in FSO systems is generally a semiconductor laser, although some manufacturers use the high power LED technology with beam collimators for that purpose. The most used semiconductors laser types are: the FP (Fabry-Perot), the DFB (Distributed Feedback) and the VCSEL (Vertical Cavity Surface Emitting Lasers).

B. Historical evolution of the semiconductor lasers

In 1960 Maiman demonstrated the performance of the first laser using a ruby crystal, operating in the visible. The first semiconductor laser, an homogeneous structure device, which used a p-n junction of GaAs, was developed in 1962 by Hall [4], [16], [17].

A perpendicular p-n junction plan with two polished end surfaces has turned the semiconductor into a small FP cavity. However, the fact that the FP lasers need a high threshold current caused heating problems in the system [18].

In 1969, was found the first solution to operate at room temperature with hetero structure semiconductor lasers, type GaAs/AlGaAs, was found.

In 1990, the need to develop laser amplifiers arose, in order to establish long haul communications using optical fibers. The need to transmit several signals simultaneously in the same physical space – Wavelength Division Multiplexing (WDM) – led to the development of DFB lasers and DBR (Distributed Bragg Reflector) lasers. This kind of lasers which transmit in one single mode increased the frequency stability of these sustems [4], [19].

Nowadays the most common laser type is the semiconductor, which has wide application. These type of lasers is usually preferred to other types, due to their great efficiency of converting electrical power into optical, their small size, light weight and possibility of being modulated directly [4], [20].

C. Types of semiconductor lasers

In the telecommunication systems the FP laser and the DFB laser are the most commonly used light sources. In the systems in which data transmission is predominant and when costs are concerned, such as the GbE (Gigabit Ethernet), the FP laser and the VCSEL are the most used [21]. In the next section a description of the composition and main characteristics of the most used types of semiconductor lasers in optical connections: the FP, the DFB and the VCSEL, is given.

a) Laser FP (Fabry-Perot)

The simplest structure of a semiconductor laser is an FP laser, as represented in Pic. 4.

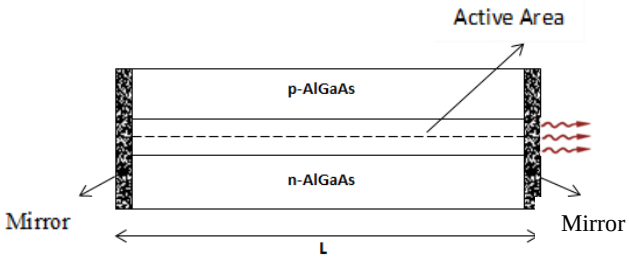

Picture 4 - Structure of an FP laser

To help confining the bearers to the active region (GaAs), the surrounding doped areas p and n, which in this case are made of AlGaAs, have a major forbidden band. In the edges two surfaces mirrors are used to control the light output on the intended edge.

The FP lasers are not composed by frequency selective elements, which means they are not Multiple-Longitudinal Mode lasers (MLM). However, by reducing the size of the cavity it is possible to get a behavior close to a single mode laser [4], [21].

b) DBF (Distributed Feedback) laser

This laser has an active area similar to that of a FP laser, with a built-in corrugation area that acts like a reflector. Instead of concentrating the reflexivity in the edges of the cavity, its reflection properties are distributed along the active area, that is, along the length of the cavity, as presented in Pic. 5.

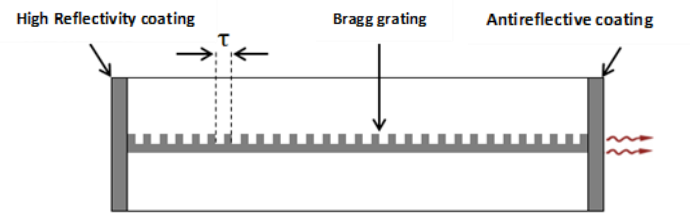

Picture 5 - Structure of a DFB laser

The reflections required for a laser operation are due to the grating, which enables only a specific wavelength. Therefore, the DBF lasers are Single Longitudinal Mode (SLM) lasers. These devices are coated with antireflective materials on the front side and with a high reflexivity coating on the rear side, in order to guarantee that the light comes out only in one direction.

c) VCSEL laser

The VCSEL laser is a single laser mode and it is geometrically different from the others. The first major difference, as we can see in Pic. 6, is that the laser transmits perpendicularly to the surface of the structure.

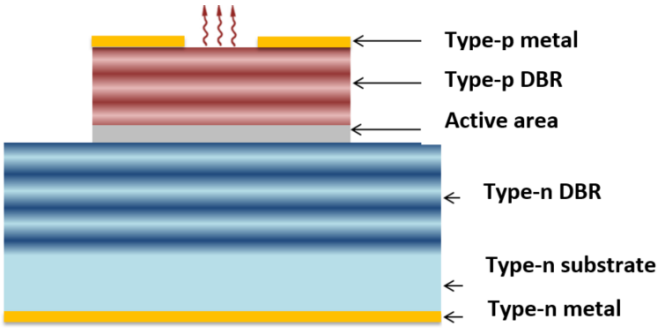

Picture 6 - VCSEL laser structure

The active area is placed between two surfaces of high reflectivity, DBR "mirrors". This high reflectivity is obtained through the formation of layers with multiple materials overlapped with different refraction indexes. [3], [22].

Table 1 presents some characteristics of the 3 types of lasers.

Parameters / Lasers	Power output (mW)	Modulation velocity	Range
FP	~2	Low	Short to medium
DFB	~20	Fast (multi-GHz)	Long
VCSEL	~4 optical ~0.5 electrical	Fast (few GHz)	Short to medium

Table 1 - Characteristics of the different semiconductor lasers

D. Modulation techniques

The modulator converts the data to transmit into a new established standardized format. Its main purpose is to obtain the maximum amount of data in the narrower bandwidth possible. There are different types of modulation schemes adequate to the FSO communication systems, such as OOK (On-Off Keying), PPM (Pulse Position Modulation) and PSK (Phase-Shift Keying) [1].

a) PSK Modulation

PSK modulation is predominant in the most recent inter-satellite optical connections and is based on the phase shifts of the modulated signal for the transmission of the different bits. The modulation techniques resulting from the PSK technique are BPSK (Binary Phase-Shift Keying), DPSK (Differential Phase-Shift Keying) and QPSK (Quadrature Phase-Shift Keying).

In the BPSK modulation each phase shift of 180 degrees corresponds to a transition of the NRZ (Non-Return-to- Zero) signal from "0" to "1" (or vice-versa, according to the previous phase).

In DPSK modulation the phase shift only occurs when a "0" bit is sent. Thus, each "0" bit sent usually corresponds to a phase variation/shift of 180º. The BPSK and DPSK techniques are shown in Pic. 7.

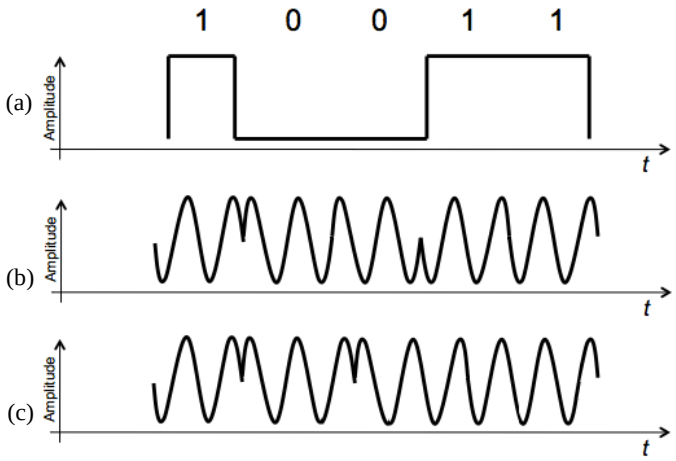

Picture 7 - PSK modulation techniques
(a) NRZ signal, (b) BPSK signal, (c) DPSK signal

In QPSK modulation it is possible to transmit bits by symbol, because phase and quadrature parameters are used in the modulated wave, making this implementation technique more complex than the previous ones.

b) OOK Modulation

OOK modulation is considered a special case of amplitude modulation. As we can see in Pic. 8, it is a binary technique in which each time lap - T_s – corresponds to a bit. The presence of a laser impulse indicates the emission of a bit "1", while the "0" bit is indicated by a null impulse (absence of signal).

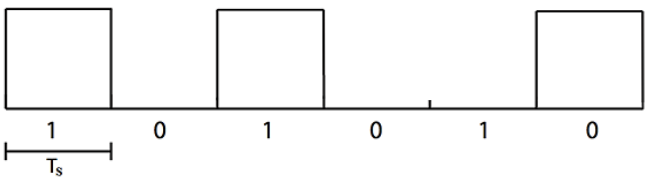

Picture 8 - OOK signal for NRZ impulses

c) PPM Modulation

M-PPM modulation consists in a time division of the transmission of a symbol in equal *M* time laps, where *M* is the modulation sequence. In order to represent a certain symbol, an impulse is sent in one of those *M* time laps, as illustrated in Pic. 9.

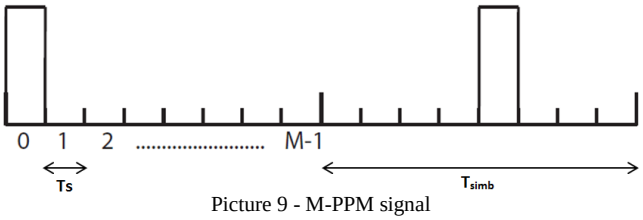

Picture 9 - M-PPM signal

IV. CIRCUITS SIMULATION AND TESTING

Two types of circuits were considered to transmit the information using the laser source. The first circuit, with discrete components, was designed to operate below 10 MHz and the second circuit, composed by integrated components, was designed to reach frequencies in the GHz band.

A. Circuit with discrete components

The first circuit was divided in three parts; the first part was composed by a differential pair, the second by two inverter stages and the third by the laser.

a) Differential Pair

The first part which can be observed in Pic. 10 is a differential pair composed by two bipolar junction transistors 2n3904 (Q1 and Q2). Their purpose is to work as differential amplifier, as both transistors are in the operation area of direct active zone.

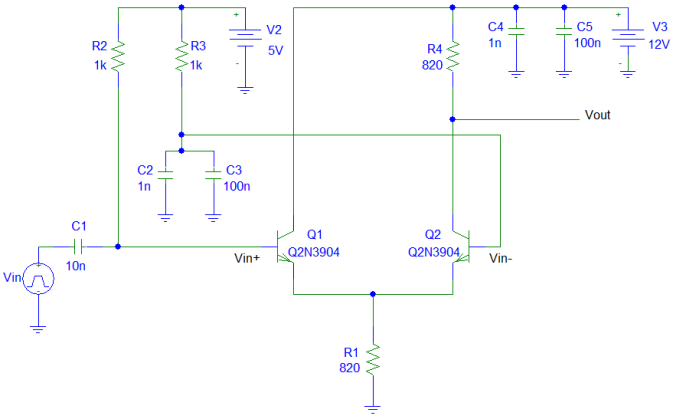

Picture 10 - Differential pair with bipolar transistors

In Pic. 11 we can see a simpler version of Pic. 10 to simplify the DC analysis of the differential pair.

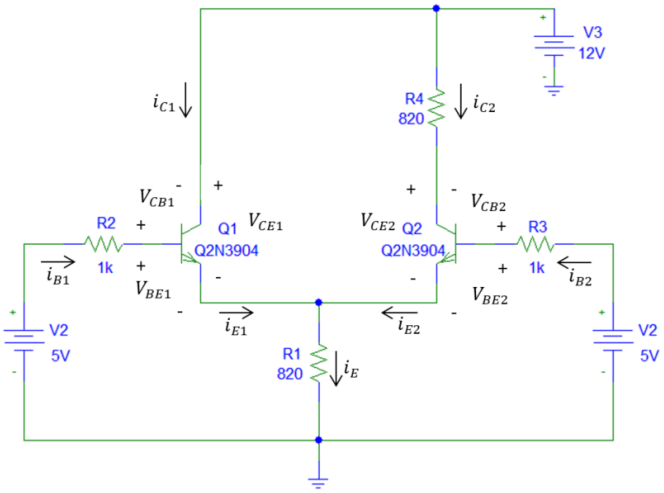

Picture 11 - Differential pair parameters

It is possible to observe all the parameters that constitute the differential pair in Pic. 11. These parameters are highly important for the theoretical calculation, enabling the interpretation of the differential pair operation. Knowing that the sum of the power failures in a closed circuit is zero, Kirchhoff Voltage Law (KVL), we can get the following expressions:

$$-5 + R2\, i_{B1} + V_{BE1} + R1\, i_E = \quad (6)$$

$$-12 + V_{CE1} + R1\, i_E = 0 \quad (7)$$

$$-12 + R4\, i_{C2} + V_{CE2} + R1\, i_E = 0 \quad (8)$$

$$-5 + R3\, i_{B2} + V_{BE2} + R1\, i_E = 0 \quad (9)$$

The sum of the currents from the TBJ Q1 and TBJ Q2 transmitters equals the current that crosses R1, that is:

$$i_E = i_{E1} + i_{E2} \quad (10)$$

Also knowing that according to the TBJ's characteristics:

$$i_{Ex} = i_{Bx} + i_{Cx} \quad (11)$$

$$i_{Cx} = \beta\, i_{Bx} \quad (12)$$

$$i_{Ex} = (1 + \beta) i_{Bx} \quad (13)$$

Admitting that $V_{BE} = 0.7\ V$ and that the current gain figure is $\beta = 200$ for both TJBs we get the differential pair parameters.

In table 2 we can see the theoretical values obtained and the values simulated in the PSpice program.

Parameter	Theoretical value	Simulation value - PSpice
$i_{B1} = i_{B2}$	13 µA	22.79 µA
i_{C1}	2.601 mA	2.626 mA
i_{C2}	2.601 mA	2.558 mA
i_{E1}	2.614 mA	2.649 mA
i_{E2}	2.614 mA	2.581 mA
i_E	5.228 mA	5.229 mA
V_B	4.987 V	4.977 V
$Vout$	9.867 V	9.900 V

Table 2 - Theoretical and simulated values

The incremental model is valid for small variations of the input signal and when the differential pair works as a linear amplifier. While in the differential mode two different voltages are applied at the base of the transisitors Q1 and Q2, respectively, $\frac{V_d}{2}$ and $-\frac{V_d}{2}$, in the common mode the tensions applied at the base, V_c are equal in both transistors.

The expressions of the differential and of the common mode gain are given, respectively, by:

$$g_d = \frac{v_0}{v_d} = -\frac{1}{2} g_m R4 \quad (14)$$

$$g_c = \frac{v_0}{v_c} = \frac{\beta\ R4}{r_\pi + 2\ (\beta + 1) R1} \quad (15)$$

with R4 = 820 Ω we can obtain a differential mode gain of $g_d = -41\ V/V$ in linear units and of $G_d = 32.26\ dB$ in logarithmic units (in module). In (15) with R1 = 820 Ω we have a common mode gain of $g_c = 0.5$ V/V in linear units and of $G_c = -6.02\ dB$ in logarithmic units.

The ratio between the differential mode gain and the common mode gain is defined as Common Mode Rejection Ratio (CMRR) and it is given by the expression:

$$CMRR = \left|\frac{g_d}{g_c}\right| \quad (16)$$

The capacity of the diferential amplifier to reject equal signals applied to the inputs Vin+ and Vin- (CMMR) amounts to 38.28 *dB*.

The TJBs used are npn type and depending on the polarization condition (direct or inverse) of each junction, they can operate in four different areas: Cut-off area, Direct or Inverse Active area and Saturation area. It was found that the colector, base and transmitter currents are equal and positive for both transistors; it was admitted that both transmitter base junctions were conducting and that the voltages at their terminals were equal to 0,7 V and that the V_{BC} voltages in the colector base junctions of the two transistors, although of different value, are both negative. In these conditions the operation area for both transistors is the direct active area.

To check the circuit's behavior the PSpice simulator was used, introducing in the circuit input a rectangular impulse ranging between 0 V and 5 V for the frequencies of 0.1 MHz and 10 MHz. In Pic. 12 we can observe the impulse for 10 MHz.

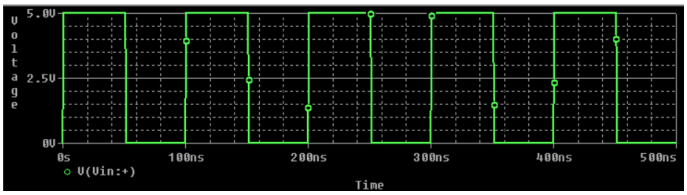

Picture 12 - Input signal Vin, 10 MHz

The signal at the output of the TBJ Q2 (Vout) colector fot the frequency of 0.1 MHz is represented in Pic. 13.

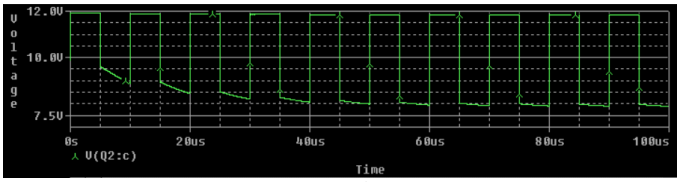

Picture 13 - Transitional regime of TJB Q2 collector, 0.1 MHz

For this frequency the signal presented in Pic. 14 was obtained experimentally.

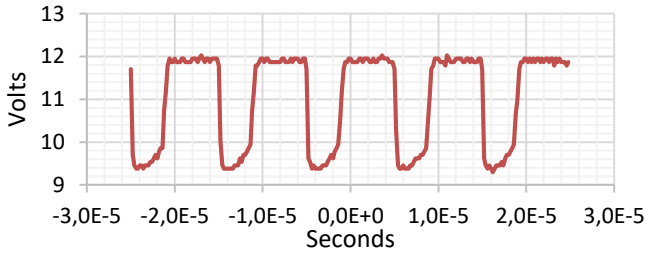

Picture 14 - Tests to the TJB Q2 collector, 0.1 MHz

Comparing the signal obtained in the experimental test with the PSpice simulation signal, we conclude that there is a slight decrease of amplitude of 0.4 V. There was also a change of the duty cycle from 50% to 75 %.

b) Inverter stages

The second part of the electrical circuit is composed by two inverter stages. Pic. 15 shows the two inverter stages in a simplified version.

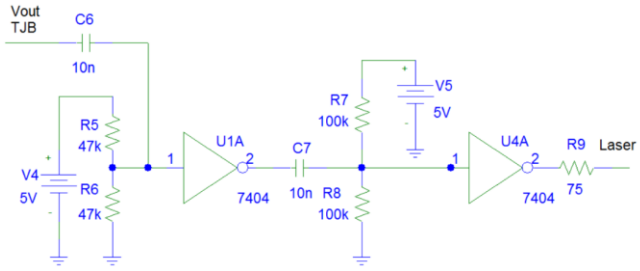

Picture 15 - Inverter stages

The two inverter stages which are part of the circuit have different roles. In both stages the inverters are connected in parallel and while the first stage, composed by 3 inverters, has the purpose of stabilizing the input signal sent from the

differential pair, the second stage, composed by 15 inverters has the purpose of supplying more current for the laser.

The signal at the output of the first inverters stage for the frequency of 0.1 MHz is represented in Pic.16.

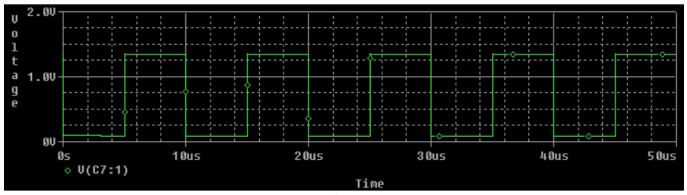

Picture 16 - Transitional regime after the 1st inverters stage, 0.1 MHz

Comparing Pic.12 with Pic. 16 the signal inversion is confirmed, however the main reason for that stage is the stabilization of the signal. I enable a constant variation between the same two levels and that it keeps a good definition in time.

The signal at the output of the second inverters stage for 0.1 MHz frequency is represented in Pic.17.

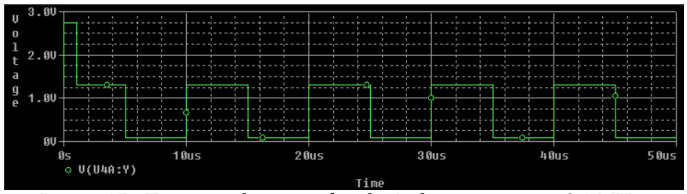

Picture 17 - Transitional regime after the 2nd inverters stage, 0.1 MHz

As we can in Pic. 17, the transitional regime of this signal is different, presenting in two time laps two different levels of voltage. The changing behavior of voltage levels is due to the voltage limits V_{1L} and V_{1H}, characteristic of the 7404 inverter. Once the V_{1L} maximum is 0.8 V and the V_{1H} minimum is 2 V, those axis were drawn in Pic. 18 chart in order to analyse the observed behavior.

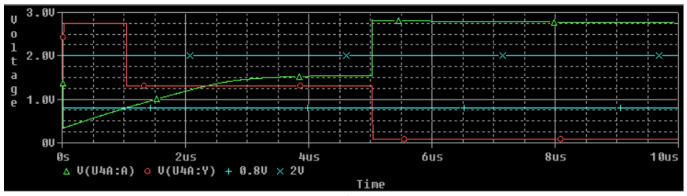

Picture 18 - Characteristics of the 7404 inverter, 0.1 MHz

Apart from V_{1L} and V_{1H} of the inverter 7404 represented in blue in the picture above, we can also see the impulse in green before the 2nd stage of inverters and in red after it. Every green signal below the V_{1L} line is considered a logical value "0", above V_{1H} line the logical value considered is "1" and between those lines there is a non-defined area.

In the experimental test as the inverters used were the 74HCT04 with different voltage levels, no problem occurred as we can see in Pic. 19.

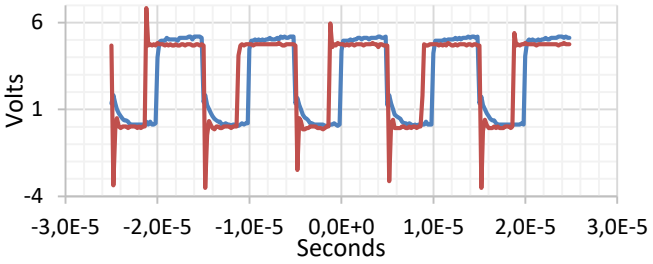

Picture 19 – Results obtained in the test to the output of the 2nd stage inverters, 0.1 MHz

We can see in the above picture that the signals are similar. In blue there is the signal introduced through a signal generator in the experimental circuit and in red the signal at the output of the second inverters stage. The red signal would be the signal to be fed to the laser.

B. Circuit with integrated components

Another way of transmitting information using a laser is by exciting it with integrated circuits of advanced technology, projected specifically for that purpose. The integrated circuits MAX3643 and DS1865 are, respectively, a circuit that controls the laser excitation current and a circuit that checks the light power transmitted by the laser and adjusts the drive current in order to keep the light power constant. Pic.20 presents the circuit which enables the information transmission with those integrated circuits, in this case projected for high frequencies.

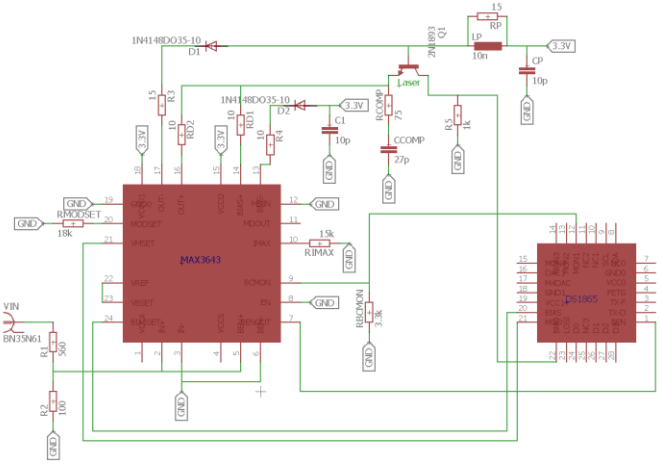

Picture 20 - Circuit for high frequencies

As we can see in Pic. 20 there are several components that involve the integrated circuit MAX3643. These are the components (resistors, capacitors and inductors) which determine the values of currents, voltages and frequencies in the circuit's operation.

Resistors R1 and R2 constitute a voltaje divider of the input signal (Vin) protecting both the integrated circuit and the laser. The signal transmitted by that voltage splitter is the input signal in the integrated circuit MAX3643, more specifically in ports IN^+ and BEN^+.

While port IN^+ is responsible for the acceptance of information bits, port BEN^+ (when active) is responsible for

the emission of light through the laser. In this case IN^+ and BEN^+ ports were connected to the same circuit point, which means that when the Vin input signal is in low level the laser is off. When the Vin input is high, the BEN^+ input enables the laser excitation according to the dimensioning performed at ports MODSET and BCMON, as we can see ahead.

Once the input maximum voltage in the integrated circuit MAX3643 (in pin IN^+) is 0.8 V, from (17) one obtains:

$$V_{IN^+} = \frac{R2}{R2 + R1} \cdot Vin \tag{17}$$

Fort he input signal Vin the same rectangular impulse was considered, but for calculation effects only its maximum value, 5 V was taken into account. Once the relation between V_{IN^+} and Vin is 0.16, the resistors values were 100 Ω for R2 and 560 Ω for R1.

Taking into account that the laser has a current threshold value of to varying between 24 mA and 30 mA and an operating current between 33 mA and 40 mA, the maximum current at the output of the integrated MAX3643, on pin IMAX (I_{MAX}) is given by (18).

$$I_{MAX} = I_{BIAS} + I_{MOD} \tag{18}$$

The current modulation, I_{MOD}, and the forward bias current, I_{BIAS}, are turned off if their sum exceeds the limit set by the resistor of the pin IMAX (R_{IMAX}). It was chosen for the current I_{BIAS} the value of 33 mA and to the current I_{MOD} the value of 5 mA. It is now possible to control the maximum current to the output of the controller by choosing appropriately the value of R_{IMAX}. For a current I_{MAX} of 38 mA the use of a resistor in the pin IMAX 15 kΩ, will prevent the laser from burning.

To be able to control both the chain of modulation I_{MOD} as the forward bias current I_{BIAS}, two resistors are introduced in the circuit, respectively R_{MODSET} and R_{BCMON}. The resistor value of R_{MODSET} can be obtained, according to the specifications of the controller MAX3643, through (19).

$$R_{MODSET} = \frac{1.2 \cdot G_{MOD}}{I_{MOD}} - R_{MOD} \tag{19}$$

where R_{MOD} and G_{MOD}, are typically 50 Ω and 88 mA/mA and denote respectively, the internal resistor of the pin MODSET and current gain modulation. The resistor value of R_{MODSET} should be chosen to produce the maximum current of modulation to the operating temperature of the laser. For a chain of modulation I_{MOD} of 5 mA, the resistor value R_{MODSET} is 21.07 kΩ. Thus, it is assumed for the resistor R_{MODSET} the value of 18 kΩ which corresponds to a chain of modulation I_{MOD} of 5.85 mA.

The resistor R_{BCMON} is obtained from the current gain of polarization, G_{BSM}, and imposing that the voltage at the terminals, V_{BCMON}, must be less than 1.4 V. The resistor R_{BCMON} is determined according to the specifications of the controller MAX3643, through (20).

$$R_{BCMON} = \frac{V_{BCMON}}{I_{BIAS} \cdot G_{BSM}} \tag{20}$$

For a current I_{BIAS} of 33 mA, with a gain G_{BSM} of 17 mA/A get a resistor R_{BCMON} of 3.03 kΩ is obtained. Thus, it is for the resistor R_{BCMON} the value of 3.3 kΩ which will have a current I_{BIAS} of 30.3 mA, higher than the stream of threshold (30 mA).

The pin OUT^+ and the pin $BIAS^+$ are the pins responsible for exit from the currents of modulation and polarization respectively. Connected to these pins, in series, one resistor of damping, R_D (R_{D1} to the pin OUT^+ and R_{D2} for the pin $BIAS^+$), increases the resistor to the passage of current through the laser. The sum of the value of this resistor with the equivalent resistor of the laser, R_{laser}, should be approximately 15 Ω. Since the typical resistor of a laser FP varies between 4 Ω to 6 Ω, it is its impedance 5 Ω, which results in a resistor R_{D1} and R_{D2} of 10 Ω.

The pins OUT^- and $BIAS^-$ allow the output of the chain of modulation and the forward bias current respectively, when the pin entry BEN is at the low level. These variations of current, lead to the pin OUT^- being connected to a resistor of 15 Ω and a diode switching diode (1N4148) the node of the laser and the pin $BIAS^-$ linked to a resistor of 10 Ω, a diode 1N4148 and a capacitor (C1) of 10 pF VCC (3.3 V), preventing the current to flow in that direction.

In the case of operation at high frequencies, a link RC (RCOMP and CCOMP) connected in parallel between the cathode of the laser and the ground, should be introduced to reduce any possible distortion in the duty-cycle of the laser, caused by their inductances parasites. It was used in this circuit to RCOMP the value of 75 Ω and for CCOMP of 27 pF, resulting in a cut-off frequency of 7.86 MHz.

To transmit data rates above 1 Gbps, it is recommended to use a link RL (RP and LP) connected in parallel between the anode of the laser and VCC. This link leads to an improvement in the response of the times of ascent and descent of the laser and reduces the instability of the same. The values of RP and LP can be adjusted taking into account the laser that is used, however, as the experimental trials in the order of GHz will be made only to confirm its operation in the high frequencies, will be used for RP and LP the values of 15 Ω and 10 nH, respectively.

V. LAYOUT OF CIRCUITS

The two circuits considered in this paper were designed in the EAGLE program, version 7.6.0, with the aim of producing each one of them in a Printed Circuit Board (PCB). The EAGLE makes the design of the electrical circuit in schematic format (*.sch*) and then finalized, generate the project in a format PCB (*.brd*).

In Pic. 21 is represented the final design for the PCB of the circuit using discrete components.

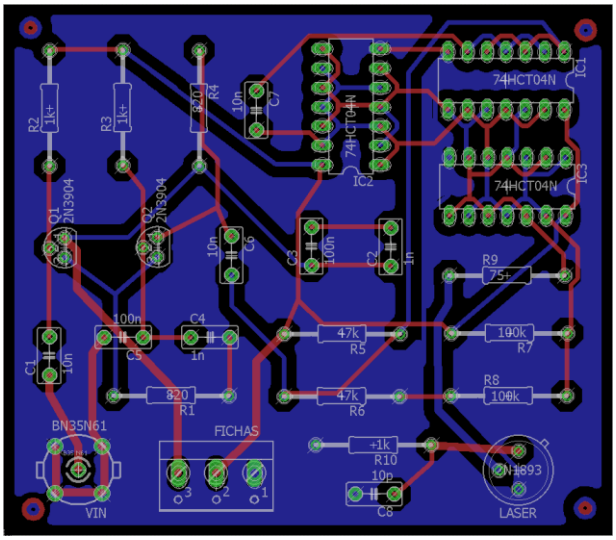

Picture 21 - First circuit PCB project

As can be seen in Pic. 21, the PCB is composed of two layers, the top layer, by red lines and the bottom layer, by the blue lines. To make a PCB design there are considerations to take into account, in particular on the width of the lines which, as can be seen in Figure, differ on connections made to the components represented by VIN, FICHAS (connectors) and LASER.

The component represented by VIN, is a male BNC connector and allows the input of a signal that will be fed to the laser. The component represented by FICHAS, has three connectors that allow to connect input signals: the port 1 signal ground (GND), in the port 2 a DC voltage of 5 V (VCC) and at the port 3 a voltage of 12 V (12VCC). These two components have links with greater bandwidth to have a lower resistor in the lines. Since the laser is a key component in this circuit, their links also have a higher bandwidth allowing quicker responses.

These two components are in Pic. 22 is represented the final design for the PCB of the second circuit with integrated components to be responsible for the excitement and control of the laser.

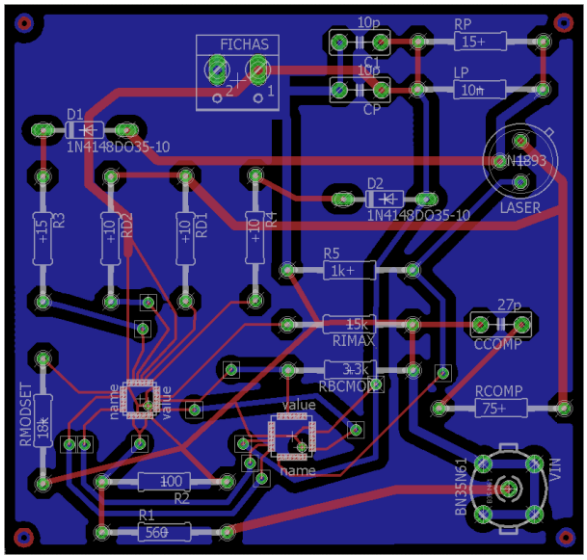

Picture 22 - Second circuit PCB project

As can be seen in Pic. 22, were taken into account the same considerations for the same components that the PCB from the first circuit. In this circuit there are only two types of signals that connect to the component FICHAS, the port 1 a DC voltage of 3.3 V that powers the integrated MAX3643 and at the port 2 signal ground (GND).

VI. Conclusions

This paper aimed at describing the optical transmitter subsystem, describe the two circuits considered, simulate the circuit in the low frequency range, designing the printed circuit boards for the two circuits and, finally, to perform experimental tests.

It was found that the FP lasers, despite having a simple structure when the size of its cavity decreases the size can obtain a behavior of a single mode laser. In this way, we used a laser FP of heterogeneous structure, AlGaInP, to establish communication on both circuits used.

In conclusion, the results obtained, were satisfactory. The main problems were the differences in the parameters of the components of PSpice simulator and experimental trials, which did not present similar results. Another problem was the inability of some electronic equipment, to operate at higher frequencies specially the signal generator and the breadboard. We were able to design a circuit with integrated components to address these constraints, whose trial is only possible with a circuit plate printed, given that those embedded MAX3643 and DS1865 have small dimensions and are of a technology (TQFN) which requires it.

The realization of this dissertation has allowed not only to acquire a wide range of knowledge in the area of optical communications optic between satellites, but also to apply the concepts that were obtained in course units over the past few years in the Military Academy and more recently at the Instituto Superior Técnico.

References

[1] H. Kaushal, G. Kaddoum, and C. Engineering, “Free Space Optical Communication : Challenges and Mitigation Techniques,” pp. 1–28, 2015.

[2] P. Major Costa, “A depência na tecnologia espacial em operações militares,” p. 83, 2013.

[3] F. S. Ujager, S. M. H. Zaidi, and U. Younis, “A review of semiconductor lasers for optical communications,” *High-Capacity Opt. Networks Enabling Technol. (HONET), 2010*, no. Cw Dm, pp. 107–111, 2010.

[4] S. Spießberger, “Compact Semiconductor-Based Laser Sources with Narrow Linewidth and High Output Power,” p. 130, 2012.

[5] J. Oscarsson, “Simulation of Optical Communication for Formation Flying Spacecraft,” no. April, p. 95, 2008.

[6] T. Tolker-Nielsen and J.-C. Guillen, “SILEX : The First European Optical Communication Terminal in Orbit,” *ESA Bull.*, vol. 96, no. november, 1998.

[7] “Satellite laser link,” *Airbus Defence and Space*, 2011. [Online]. Available: http://www.space-airbusds.com/en/news2/satellite-laser-link.html. [Accessed: 05-Aug-2016].

[8] “First image download over new gigabit laser connection in space,” *Airbus Defence and Space*, 2014. [Online]. Available:

https://airbusdefenceandspace.com/newsroom/news-and-features/first-image-download-over-new-gigabit-laser-connection-in-space/. [Accessed: 05-Aug-2016].
[9] D. Stillman, “What is a Satellite?,” 2014. [Online]. Available: http://www.nasa.gov/audience/forstudents/5-8/features/nasa-knows/what-is-a-satellite-58.html. [Accessed: 06-Aug-2016].
[10] H. Riebeek, “Catalog of Earth Satellite Orbits,” *NASA - Earth Observatory*, 2009. [Online]. Available: http://earthobservatory.nasa.gov/Features/OrbitsCatalog/. [Accessed: 06-Aug-2016].
[11] G. Brown and W. Harris, “Types of Satellites,” *How Satellites Work*. [Online]. Available: http://science.howstuffworks.com/satellite7.htm. [Accessed: 06-Aug-2016].
[12] C. Tenente-Coronel Mendes Dias, “O Espaço na Guerra Futura,” *Rev. Mil.*, vol. 2453/2454, pp. 1–39, 2006.
[13] H. Henniger and O. Wilfert, “An introduction to free-space optical communications,” *Radio Eng.*, vol. 19, no. 2, pp. 203–212, 2010.
[14] M. A. Khalighi, M. Uysal, C. Marseille, and E. Engineering, “Survey on Free Space Optical Communication: A Communication Theory Perspective,” *IEEE Commun. Surv. Tutorials*, vol. 16, pp. 2231–2258, 2014.
[15] P. Singal, S. Rai, R. Punia, and D. Kashyap, “Comparison of Different Transmitters Using 1550nm and 10000nm in FSO Communication Systems,” *Int. J. Comput. Sci. Inf. Technol.*, vol. 7, no. 3, pp. 107–113, 2015.
[16] J. Mulet, “SEMICONDUCTOR LASER DYNAMICS. Compound- cavity, polarization and transverse modes,” no. December, p. 248, 2002.
[17] “The biography of Theodore Maiman,” *Laser Inventor-Creator of the World’s first laser*. [Online]. Available: http://www.laserinventor.com/bio.html. [Accessed: 07-Aug-2016].
[18] S. B. Alves, “Dinâmica em frequência de laser semicondutor sob realimentação ótica ortogonal filtrada,” Federal da Paraíba, 2012.
[19] S. W. Koch, Weng W.; Chow, *Semiconductor-Laser Fundamentals, Physics of the Gain Materials*. Berlin: Springer, 1999.
[20] G. S. Oliveira, “Formatos de Modulação de uma Portadora Óptica com Detecção Direta,” pp. 1–89, 2011.
[21] E. Sackinger, “Optical Transmitters,” *Broadband Circuits Opt. Fiber Commun.*, vol. 1, pp. 233–257, 2005.
[22] J. O. Carroll, “Novel Optical Transmitters for High Speed Optical Networks,” Dublin City University, 2013.

João Trindade was born in Sines, Portugal, on August 16, 1991.

In 2010 he joined the Portuguese Army where he completed the Bachelor degree in Telecommunications at the Military Academy, in Lisbon. Currently, he is attending a Master’s degree course in Electrical and Computer Engineering at Instituto Superior Técnico, Lisbon.